

Strengthening of Reinforced Concrete Flat Slabs to Resist Punching using Different Techniques

Hanna F. H. Habeb¹, Ahmed A. Mahmoud*², Alaa G. Sherif³, Magdy M.M. Genidi⁴

*Corresponding author, E-mail: ahmed.ahmed@feng.bu.edu.eg,
ahmed.m5882@gmail.com

Department of Civil Engineering, Faculty of Engineering at Shoubra, Benha University-

, 108 Shoubra Street, Shoubra 11691, Cairo, Egypt.

1- Higher Institute of Engineering, 15th of May City, Egypt (E-mail: civil.hanafakhry@yahoo.com).

Professor, Faculty of Engineering (Shoubra), Benha University, Egypt (E-mail: ahmed.ahmed@feng.bu.edu.eg and ahmed.m5882@gmail.com);

2- Professor of Reinforced Concrete Structures, Civil Engineering Dept., (Structure), Faculty of Engineering El Matarya- Helwan University, Cairo, Egypt (E-mail: alaa_sherif@m-eng.helwan.edu.eg and agbsherif@gmail.com);

3- Associate Professor, Civil Engineering Dept., (Structure), Faculty of Engineering El Matarya- Helwan University, Cairo, Egypt (E-mail: magdy_genedy@m-eng.helwan.edu.eg and magdy_genidi@yahoo.com).

ABSTRACT

Failure of reinforced concrete flat slabs due to punching is very interested subject. The major purposes of this study are to study experimentally, analytically and numerically the effectiveness of the proposed external strengthening techniques to resist punching shear of reinforced concrete flat slabs. The used external strengthening techniques were: (1) external drop panel confined with GFRP sheets, (2) external steel shear studs (Bolts) at different distances (at half slab effective depth and at the slab effective depth from the column face), (3) external GFRP stirrups, at different distances (at half slab effective depth and at the slab effective depth), and (4) external GFRF sheet in the compression side. The experimental program consisted of seven square specimens (1700 x 1700 x 150 mm) with circular column (stub) had 250 mm diameter at its center. The tested specimens are intended to simulate a half scale interior-slab-column connection. All specimens tested as simply supported slabs under one-point static loading at the center of the column. The numerical program was carried out using ANSYS V.19 as nonlinear finite element software program to study the influence of studied parameters. Calibration and verification of ANSYS V. 19 has been done by comparing the results of the load deflection curves, cracks and ultimate loads with the experimental ones. The results showed that both ECP 203-2017 [1] and ACI 318-19 [2] building codes are conservative compared to the experimental results.

The results show that, using external strengthen by GFRP stirrups and steel shear studs (Bolts) on circles located at distance half the slab effective depth and at the slab effective depth after the column face is an effective method to improve: (1) the ultimate punching shear load, (2) maximum deflection, (3) displacement ductility, (4) toughness, (5) secant stiffness, (6) cracks patterns and (7) failure modes.

Key words: Punching shear; Flat slabs; Experimental; External strengthening.; ANSYS program; Numerical analysis; Load- deflection; Ultimate load; Cracks patterns; Cracking load; Yielding load; Failure modes; Secant stiffness; Toughness; Displacement ductility and Strains.

HIGHLIGHTS

- Description of the experimental investigation conducted for seven reinforced concrete slabs to the effect of external strengthening to resist punching;
- Studying the behavior of reinforced concrete flat slabs externally strengthened using different techniques;
- Studying the effect of using external steel shear studs (Bolts), external GFRP stirrups at different distances on the ultimate punching shear resistance of reinforced concrete flat slabs;
- Evaluating the failure modes and crack patterns; and
- Analyzing the experimental results of RC flat slabs externally strengthened and giving and providing recommendations for designer and site engineers.

1. Introduction

Uses of flat slabs systems are becoming popular in most construction project. Flat slabs are suitable to most floor cases and usage. Flat slab system is from the important systems that allow more freedom for architectural purposes. Flat slab is frequently the best optimal when we need open spaces such as theaters and high rise buildings. It given architectural suppleness, more clear area, reducing the height of building and, therefore less time to construct the building.

The brittle punching failure it is dangerous problem that appear in flat slabs due to transfer of shearing forces occurs without warning in flat slabs. When loading with a heavy vertical load on the column connected to the flat slab, cracks will arise within the slab close to the column. Punching failure occurs when the shear stresses are too high when loading with a large vertical load in the slab area around the column.

One of the main methods used in flat slabs for raise the punching shear strength of flat slabs[3]: (1) column head or drop panel a is made around the region column raise thickness the slab, (2) using steel sections or steel plates, steel studs, stirrups for consolidation of the slab column connection to resist punching shear stress, and (3) using GFRP sheets to improve the shear executions [3-7].

There is large effect on the load-deflection characteristics of the specimens subjected to high-moment as a result of the use of high strength concrete slab [8-10].

There are many researches studies that have examined the effect of main shear reinforcement [11-12]. It was observed through those studies is a clear influence on the punching shear behavior a result of the percentage of flexural reinforcement in presence of shear reinforcement.

Shear reinforcement prevents propagation of shear cracks, reduce crack width and punching shear capacity [13-18].

The steel fibers are very impressive in changing brittle punching failure to ductile flexural failure, through increasing both the ultimate load and deflection, as long as strengthen fiber reinforcement is guaranteed [19-20]. The steel fibers and steel shear studs have great impact resistance punching shear.

There are many researches that talk about finite element and analytical study [21-24].

There are also many practical experiments conducted to know the influence of many factors on resistance punching shear [25]. Prestressed carbon fiber-reinforced polymer straps and post tension prevent propagation of shear cracks and increase consolidation of flat slabs for resistance punching shear [26-27].

Nomenclature

$A_{S_{Bottom}}$: the tension main steel reinforcement ($10\Phi 16/m^2 = 17$ bar (constant));

$A_{S_{top}}$: the compression secondary steel reinforcement ($5\Phi 10/m^2 = 9$ bars (constant));

FRP and GFRP: Fiber and Glass Fiber Reinforced Plastic;

d : the slab effective depth (= total depth – concrete cover (20 mm) = 130 mm (constant));

t_s : the slab total thickness (150 mm (constant));

P_{cr1} , P_{cr2} , P_u and Δ_u : the first, the second crack load, the ultimate load and the deflection at ultimate load.

P_y : the yield load of the main steel reinforcement at $\epsilon_y = f_y/E_s = 0.0018$ ($f_y = 360$ MPa and $E_s = 2 \times 10^5$ MPa);

ϵ_1 and ϵ_2 : the average strain of the main steel reinforcement in directions x and y at the ultimate load;

D.D (Displacement ductility) (-): is the ratio of the deflection at 90 % of the ultimate load in descending branch (after the ultimate load) to that in the ascending branch (before the ultimate load);

f_{cu} and f_c : the cubic and the cylindrical concrete compressive strength (26 MPa and 22 MPa respectively);

$P_{cr\ exp.}$ and $P_{u\ exp.}$: the experimental first crack and ultimate load;

$P_{cr\ Num}$ and $P_{u\ Num}$: the predicted first crack and ultimate load from numerical analysis; and

$\Delta_{u\ exp.}$ and $\Delta_{u\ Num}$: the experimental and the predicted deflection at ultimate load.

2. Experimental program

In this study the experimental program performed using external strengthening techniques to resist punching shear of reinforced concrete flat slab systems.

2.1 Description of tested slabs

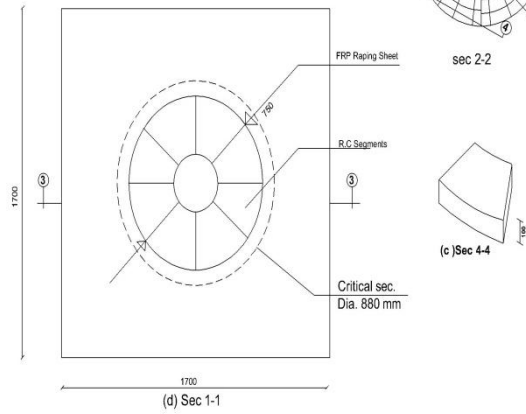
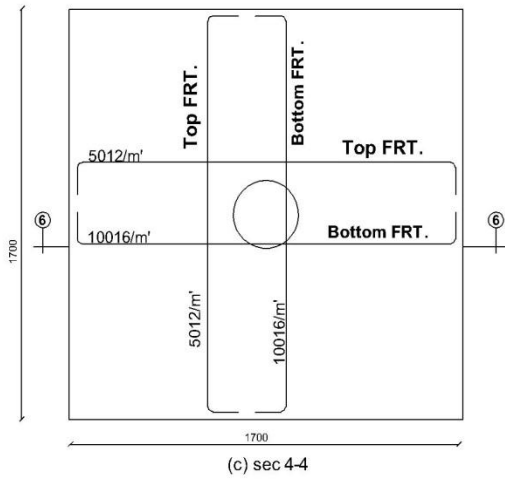
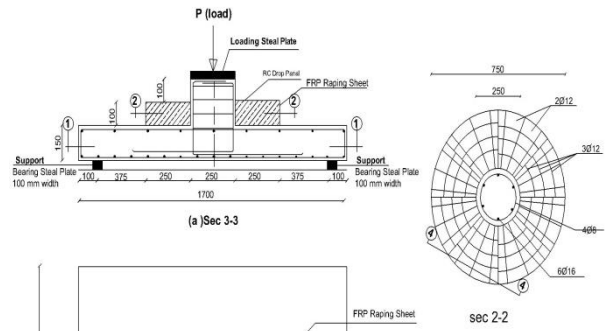
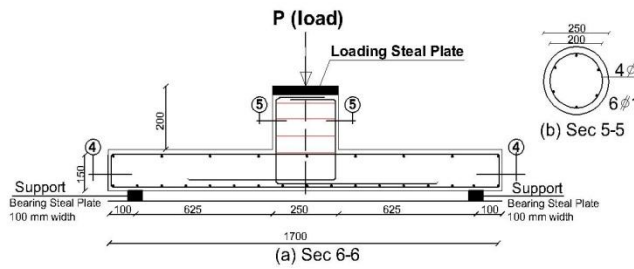
All specimens had the same amount and placement of orthogonal longitudinal reinforcement details as shown in Figs. 1 and 2. All specimens are of constant dimensions (1700 mm× 1700 mm) with 150 mm thickness. The study includes seven specimens with an upper central circular column 250 mm diameter and 200 mm height. All specimens were tested and loaded in the lab as simply supported slabs under one-point static loading at the center of the column.

The first specimen S1 is the control specimen without any strengthening. The second specimen S2 strengthened using external drop panel segments confined with GFRP sheets. The third specimen S3 strengthened using external steel shear studs (Bolts) located on a circle at a distance half the effective slab depth ($0.5 d_{slab}$) from the column face. The fourth specimen S4 strengthened using external steel shear studs on two circles at distances ($0.5 d_{slab}$ and d_{slab}) from the column face. The fifth specimen S5 strengthened using external GFRP stirrups located on circle at a distance $0.5 d_{slab}$ from the column face. The six specimen S6 strengthened using external GFRP stirrups on two circles at distances ($0.5 d_{slab}$ and d_{slab}) from the column face. The seventh specimen S7 strengthened using external GFRP sheet in the compression side.

The concrete used has an average cubic compressive strength of 26 MPa as a result from twelve different concrete mixes using standard cubs (150 x 150 x150 mm). The mechanical properties of concrete are shown in Fig. 3. The specimens were reinforced with flexural reinforcement ($A_{s\text{ Bottom}}=10\phi 16/m^2$ and $A_{s\text{ top}}=5\phi 12/m^2$) and circular column reinforced with (6 ϕ 16) with 4 ϕ 8 mm rings. The properties of the reinforcement steel are shown in Table 1 and Fig. 4. Proper concrete cover was maintained and the process was under guidance of professional bar benders.

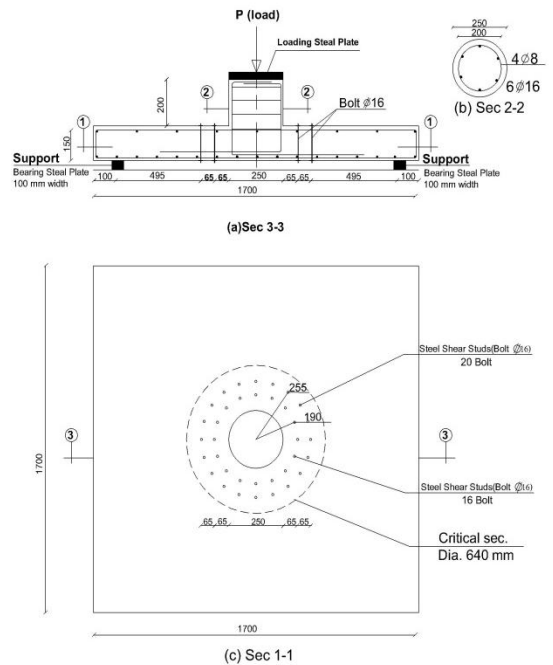
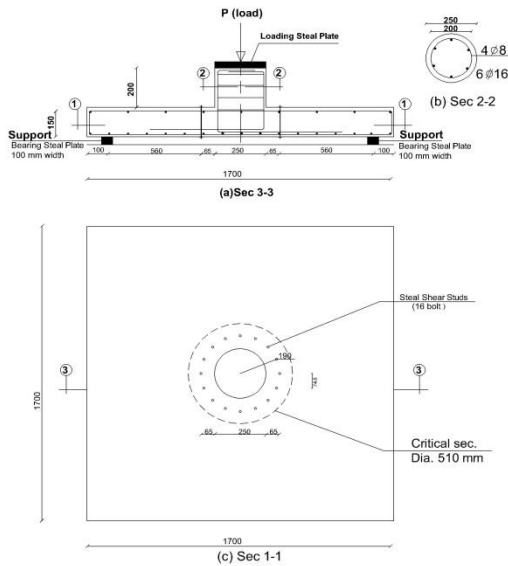


Figure 1 Typical arrangement of slab reinforcement.



(a) Reinforcement details of all specimens

(b) Specimen S2



(c) Specimen S3

(d) Specimen S4

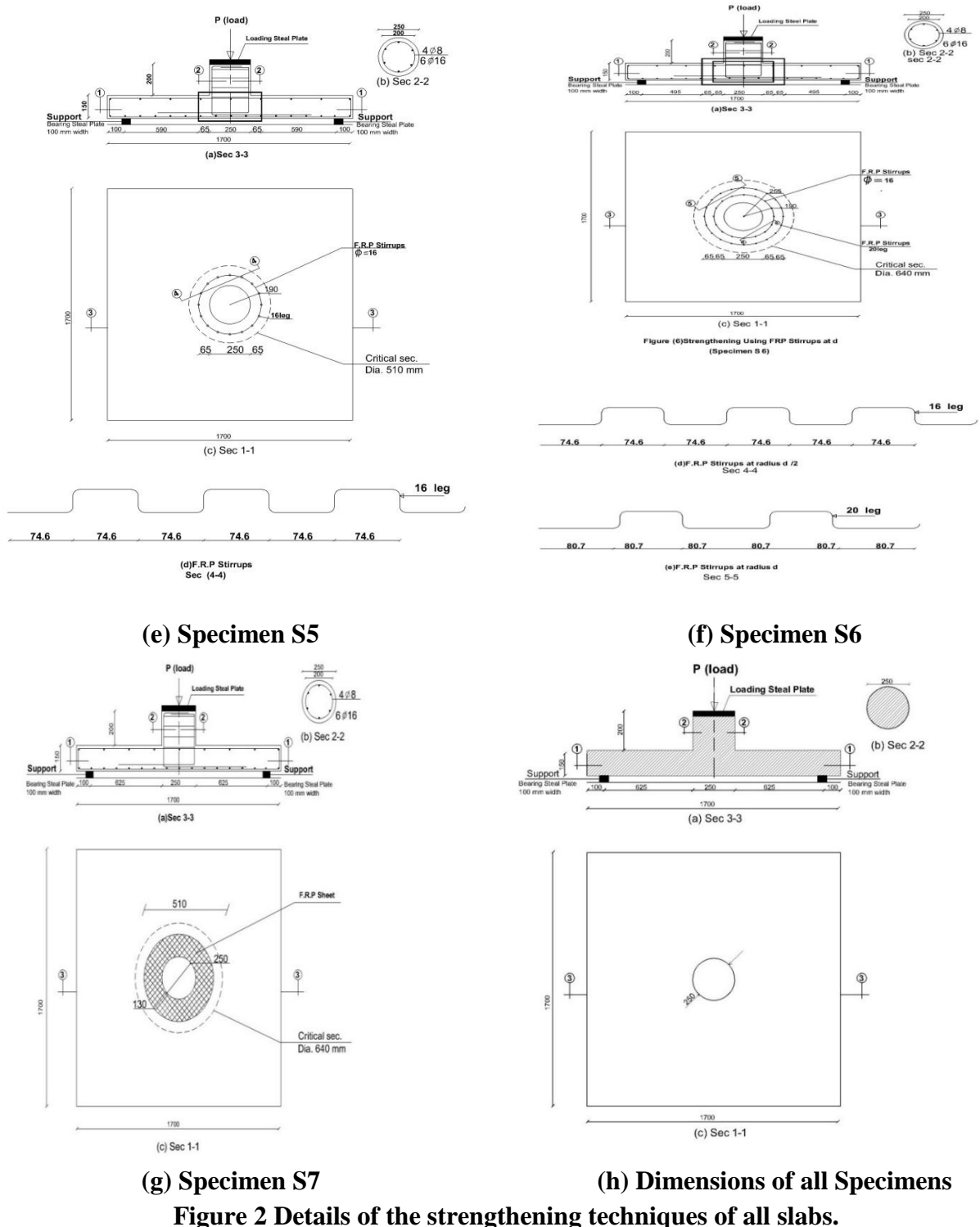


Table 1: Mechanical properties of the reinforcement steel bars.

Diameter (mm)	Actual Area* (mm ²)	Yield Strength (MPa)	Strain at yield strength, ϵ_y	Ultimate strength, f_u (MPa)	Elongation %	Young's modulus, E_s (GPa)
8	48.40	334	0.00172	463	15.4	195

10	78.40	553	0.00276	699	13.8	200
16	197.88	550	0.00275	706	12.0	200

* Actual area= weight of a certain length of reinforcement steel bar/ (Bar length * steel reinforcement specific weight).

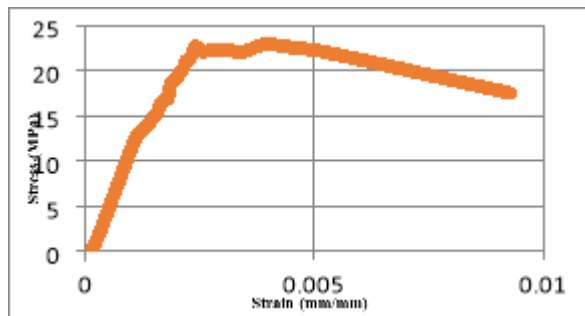


Figure 3 Concrete compressive stress-Strain curve for tested slabs.

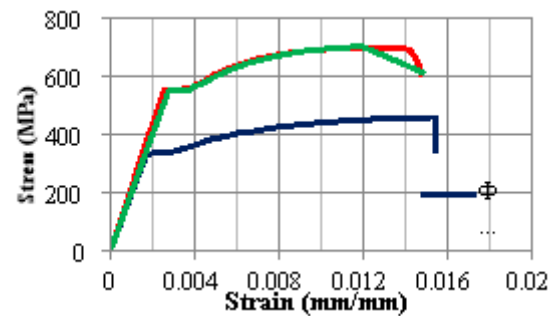


Figure 4 Steel reinforcement stress-strain curves

2.2 Materials properties

The tested slabs and mix were designed according to the ECP 203 -2017 [1] and ACI 318-19 [2]. The mix proportion by weight of the amounts for one m³ of concrete to accomplish the objective compressive strength were 350,690,1110 and 179 Kg for the Ordinary Portland Cement (OPC), sand, aggregate and water respectively and specific gravity of the used materials were 3.15,2.61,2.67 and 1.0 respectively. Coarse aggregate with 10 mm maximum size was used. The average cubic and cylindrical concrete compressive strength were 26 and 22 MPa, respectively.

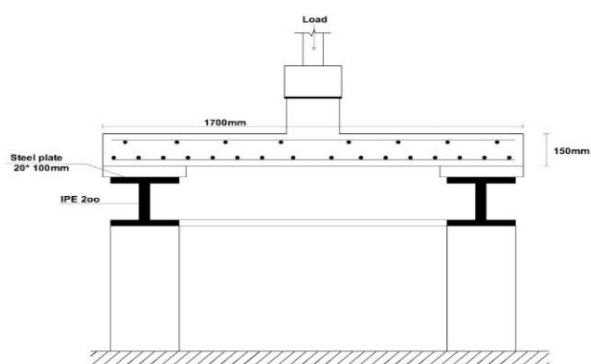
The used steel shear studs (bolts) have diameter 16 mm with strength 500 MPa. Thixotropic impregnating adhesive was used to resin / adhere the fiber reinforcing fabric and drop panel. Epoxy (Sikadur -165) was used in this experimental program. The used GFRP had strength 1100 MPa. The tensile strength for steel reinforcement bars was determined according to test method B.2 in ACI 318-19 [2]. Mechanical properties of the reinforcement steel are shown in Table 2.

2.3 Instrumentation, test set up and test procedure

External measuring apparatuses were attached to the specimen in order to obtain the overall deformations, applied vertical loads. Deflection was measured by Linear Variable Differential Transducers (LVDT) connected to the specimen as displayed in Fig. 5. The load cell and LVDTs were involved to data logger system in order to record all results through the test stages. Before starting the test, the load cell and LVDT were calibrated then their initial values were reset to zero through the lab program. The specimen was located and axis of applied load was aligned with the machine axis to achieve the specific required horizontal distances. Four electrical strain gauges with a gage length of 10 mm were used for each specimen to measure the strains in the longitudinal bottom steel reinforcement, two in the X-

direction and two in the Y-direction. The readings of the electrical strain gauges were recorded in order to determine strains in flexural reinforcement.

The specimens were loaded using one load cell, has a capacity of 500 kN. Figure 5 displays the used typical test setup. As shown, the load cell was attached to the testing frame by plates and high strength steel bolts. The load was applied as a monotonic static load increasing under displacement control. The cracks are marked at each load increase. The specimens were supported all around on hinged support assembled from steel plate with 20 mm thickness and 100 mm width rested on steel I-section (IPE 200).



(a) Elevation view of the test setup.

(b) Photo of the test setup and instrumentations.

Figure 5 Test set-up and instrumentations.

3. Analysis of the experimental results

This study presents all the measured test results, such as: (1) the relation between the load and the deflection at left, middle and right of the specimen, (2) the relation between the load and the reinforcement strains, (3) ultimate load, (4) cracks patterns, (5) cracks width and (6) failure modes. Table 2 displays the experiment results for all the tested specimens.

Table 2 Experimental results.

Slab No.	P_{cr1} (kN)	P_{cr2} (kN)	P_y (kN)	P_u (kN)	Δ_{cr1} (mm)	Δ_{cr2} (mm)	Δ_u (mm)	ϵ_x ($\times 10^{-6}$)	ϵ_y ($\times 10^{-6}$)	S.S (kN/m)	D.D (-)	T (kN.m)	Failure Modes
S1	135.18	201.52	343.43	351.01	7.876	10.906	20.386	1930	1795	17.218	1.28	3319.1	Punching-shear

S2	191.35	291.31	495.12	535.63	11.822	16.693	30.485	2240	2040	17.570	1.32	7973.9	Punching-shear
S3	184.85	285.88	497.58	536.12	8.090	11.789	31.056	2311	2138.5	17.263	1.74	6029.7	Punching-flexural
S4	243.62	387.27	518.87	591.10	12.349	18.192	32.651	2497	2199.5	18.104	1.63	8437.4	Punching-flexural
S5	189.45	288.14	511.68	562.37	13.028	19.068	32.374	2330	2170	17.371	1.40	10329.2	Punching-flexural
S6	250.37	406.01	556.86	657.29	18.337	26.293	36.293	2586	2398.5	18.411	1.40	13821.2	Punching-flexural
S7	146.12	233.49	376.25	387.08	9.783	13.886	22.455	1965	1830	17.238	1.30	4478.6	Punching-shear

Table 3 Experimental results compared to the control specimen (S1)

Slab No.	$\frac{P_{cr1}}{P_{cr1S1}}$ %	$\frac{P_{cr2}}{P_{cr2S1}}$ %	$\frac{P_y}{P_{yS1}}$ %	$\frac{P_u}{P_{uS1}}$ %	$\frac{P_y}{P_u}$ %	$\frac{\Delta_u}{\Delta_{uS1}}$ %	$\frac{\epsilon_x}{\epsilon_{xS1}}$ %	$\frac{\epsilon_y}{\epsilon_{yS1}}$ %	$\frac{S.S}{S.S_{S1}}$ %	$\frac{D.D}{D.D_{S1}}$ %	$\frac{T}{T_{S1}}$ %
S1	100	100	100	100	98	100	100	100	100	100	100
S2	142	145	144	153	92	150	116	114	102	103	240
S3	137	142	145	153	93	152	120	119	100	136	182
S4	180	192	151	168	88	160	129	123	105	127	254
S5	140	143	149	160	91	159	121	121	101	109	311
S6	185	201	162	187	85	178	134	134	107	109	416
S7	108	116	110	110	97	110	102	102	100	102	135

3.1 Load deflection curves and ultimate loads

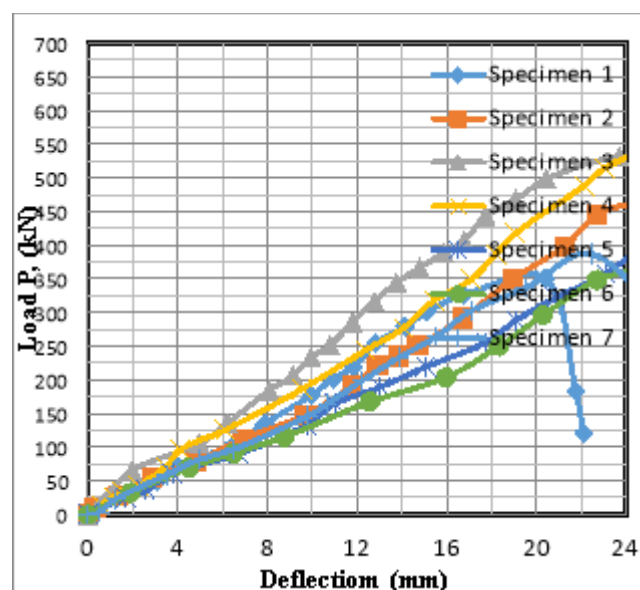
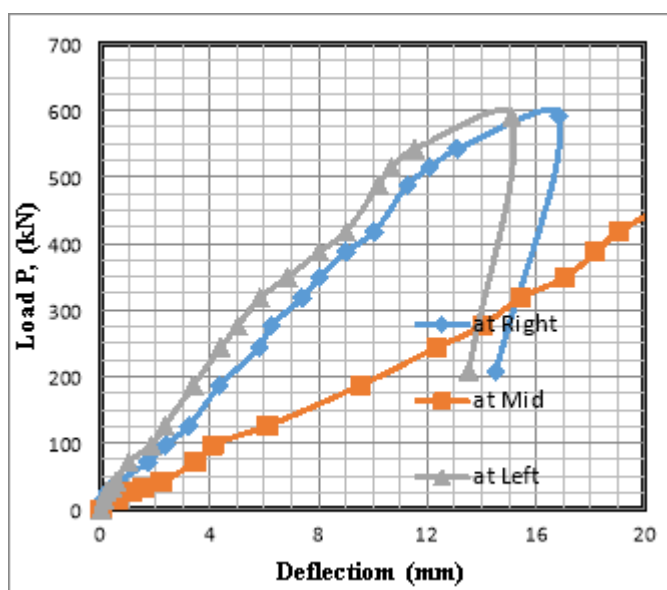
The experimental load–deflection curves for the seven specimens are plotted in Fig.6. All figures show the values of the deflection at right, mid and left of the specimen. It is clear that deflection increases with increasing load until reached the ultimate load. Large deflection occurred at mid of the specimen (under the column). The left and the right LVDTs were almost has the same values due to symmetry. After reaching ultimate load, load decreased while deflection increased. The secant stiffness, toughness, and displacement ductility calculated from the load–deflection curves are shown in Tables 2 and 3.

Generally, the shape of load–deflection curves the beginning is linear it appears the initial cracks then linear which occur at the yield of the longitudinal main reinforcement after that the load decreases and deflection increases through for consecutive loads.

Obviously using external strengthening increases the ability of the slab to resist punching shear and a higher ultimate load accompanied with more deflection can be obtained as shown in Fig.6. Additionally, the slab took longer time to fail in punching failure. It can be noticed that, the use of external strengthened with steel shear studs (Bolts) on two circles at distances $d/2$ and d from the column face (Specimen S4) has better deflection than that use of steel shear studs (Bolts) on circle at distance $d/2$ (Specimen S3) where the deflection at the ultimate load increased by 15 % while the use of external GFRP stirrups at distances ($d/2$ & d) from the face of the column (Specimen S6) is better than use of GFRP stirrups on circle at distance $d/2$ from the column face (Specimen S5) where the deflection at the ultimate load increased by 12 %.

There was significant improvement in the deflection at the ultimate load recorded for slabs with GFRP stirrups or steel shear studs (Bolts) at ultimate compared to the control specimen. Also, for specimens has two rows of GFRP stirrups or two rows of steel shear studs (Bolts) more deflections were observed than in the specimen has only one row or the slab without GFRP stirrups or steel shear studs (Bolts) which means more ductile failure.

After reaching ultimate load, load decreased and deflection increased under the column while the deflection at the right and at the left part of the column decreased due to punching failure where the middle part goes down and the left and the right parts go up as shown in Fig.7.



(a) Specimen S4 (as example)

(b) All Specimens

Figure 6 Load- deflection curves of the tested specimens.

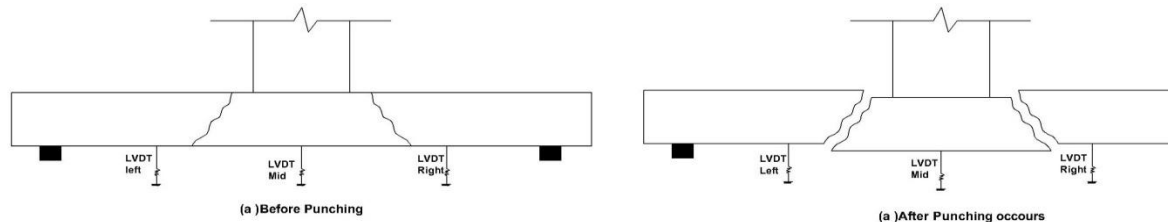


Figure 7 Deformed shape of the slab.

3.2 First crack load and cracks pattern

In general, it was noted that before reaching the ultimate load that all specimens exhibited similar cracks pattern. With the spread of the cracks pattern, very fine tangential cracks appeared where start crack noticed around the column then a number of fine cracks moved into radial shapes whose path from the column faces toward the slab edges. By increasing the load more tangential cracks formed at larger radii. It was observed that the specimens provided with external strengthening had a similar behavior in the spread of cracks, especially slabs with shear reinforcement which has more intense crack dissemination and larger failure loads. Typical cracks pattern is shown in Fig.8.

Generally, the cracks were first noticed in the tension face of the slab along and perpendicular to the edges of the column. The first crack loads are shown in Table 2. The first crack at the tension side (lower face) starting from the column and extending a short distance towards the supports. As the slab is further loaded, more cracks appeared in the slab. The cracks showed on the upper face of the slab (compression side) about the column and starting to propagate along the supports. Cracks width increased due to the load increases where the cracks started to spread along all directions of the tested slab. The tangential and radial cracks widened and dense propagation at the approaching failure load. Figure 9 displays the cracks pattern of all tested samples. It was noticed from the crack patterns, that all slabs were affected by nearly similar cracks pattern. The radial cracks were the most obvious and continuous ones, but the main difference was in the distribution and number of the fine cracks.

At the occurrence of first and second crack, the corresponding first and second crack load were recorded and the cracks pattern were plotted. Table 2 summarizes the observed test results of all samples tested and Table 3 shows the results compared to the control sample S1. The experiment results displayed that the first crack load (P_{cr1}) was enhanced due to using external strengthening, where the first crack load (P_{cr1}) increased by 42%, 37%, 80%, 40 %, 85% and 8% respectively for samples S2, S3, S4, S5, S6 and S7 compared to the reference sample S1, while the second crack load (P_{cr2}) increased by 45 %, 42 %, 92 %, 43 %, 101 % and 16 % respectively.

It was observed that the tested specimens S3, S4, S5 and S6 had crack width limited to 1 mm to 2 mm less than the control specimen S1 which means that the shear studs (Bolts) and GFRP stirrups effectively prevented propagation of shear cracks. Also, the results show that

using of two rows of steel shear studs (Bolts) or GFRP stirrups effectively prevent propagation of shear cracks and reduce crack width compared to the specimen using one row.

From Tables 2, and 3, it can be concluded that the external strengthening increases the deflection at the first and second crack (Δ_{cr1} and Δ_{cr2}) which means increase the secant stiffness (load/deflection i.e. the slope of the ascending branch of the load-deflection curve (kN/mm)) and increase displacement ductility.

From Table 3 it can be concluded that the first and the second crack load for specimens S2, S3 and S4 has almost the same range (37 % to 45 %) of the ultimate load while these values ranging between 80 % to 101 % for specimens S4 and S6. Insignificant enhancement was observed for the first and second crack load when use external GFRP sheets in the compression side (Specimen S7).

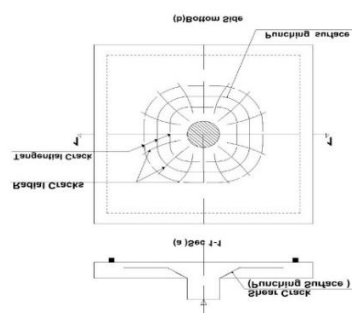


Figure 8 Typical cracks pattern for concrete due to punching.

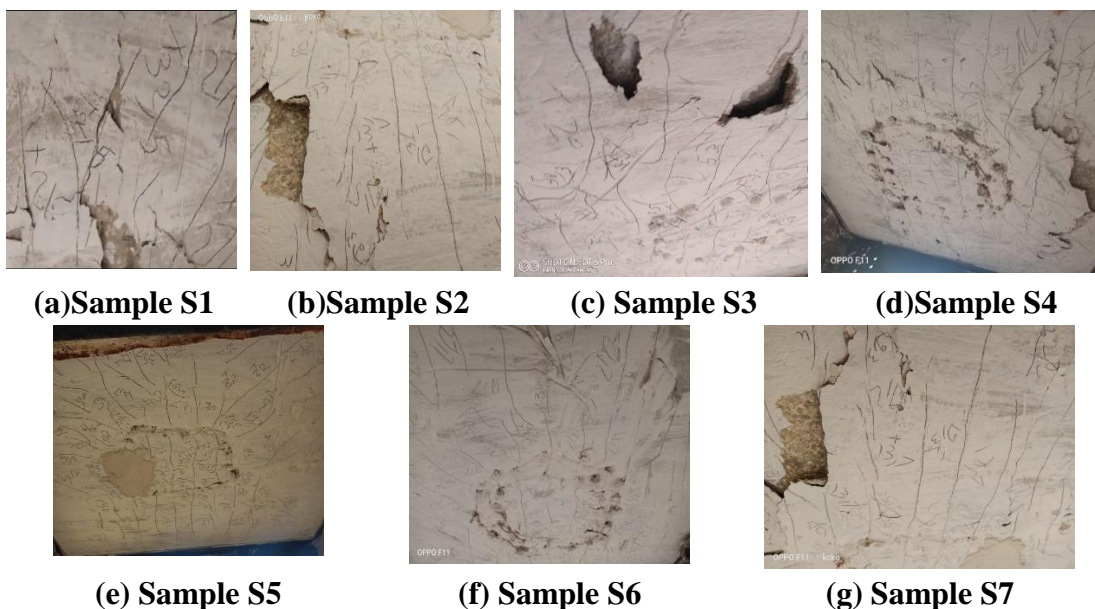


Figure 9 Cracks pattern of all tested samples.

3.3 Failure modes

In this study, slabs failed in punching shear failure mode and punching-flexural failure mode as common in flat slabs as shown in Fig. 10 and Table 3. At failure, there was a complete loss of stiffness observed by the sudden drop in load and appearance of cracks in the compression face at top slab parallel to the column face. Separation of the concrete cover

(tension side) for the lower part of the slab. The reinforcement was appeared and parts of concrete fell on the ground as the sample failed in punching outside of the shear reinforcement zone.

Sudden brittle failure occurred for slabs S1, S2 and S7 around the column with the forming of a sectioned cone in the slab and the failure mode was punching shear, while specimens S3, S4, S5, and S6 failed in punching-flexural failure which means that the use of steel shear studs (Bolts) and GFRP stirrups on circles at distance $d/2$ and at distances $d/2$ and d from the column face variation the failure type from punching failure to punching-flexural failure.

For slab S2 and as a result of the consolidation, the ability of the slab to resist punching increased. Additionally, the slab took longer time for punching shear failure mode to occur and sudden brittle failure happened after the drop panel zone about the column with the forming of a sectioned cone in the slab.

For slabs S3 and S5, punching occurs after a distance $d/2$ from the column face and the failure mode was punching- flexural failure. There was significant improvement in the maximum deflection recorded for slabs with GFRP stirrups or shear bolts as shear studs before failure compared to the reference sample without shear bolts (S1).

For slabs S4 and S6 punching failure occurs after a distance d from the column face, and the failure mode was punching- flexural. At failure, it can be noticed that using steel shear studs (bolts) or GFRP stirrups occasioned in less prevalent cracks and less crack width. For slab S6, it can be noticed that, the use of GFRP stirrups instead of steel shear studs (Bolts) is better not only in resentencing punching but also in reducing the deflection, cracks width and cracks propagation.

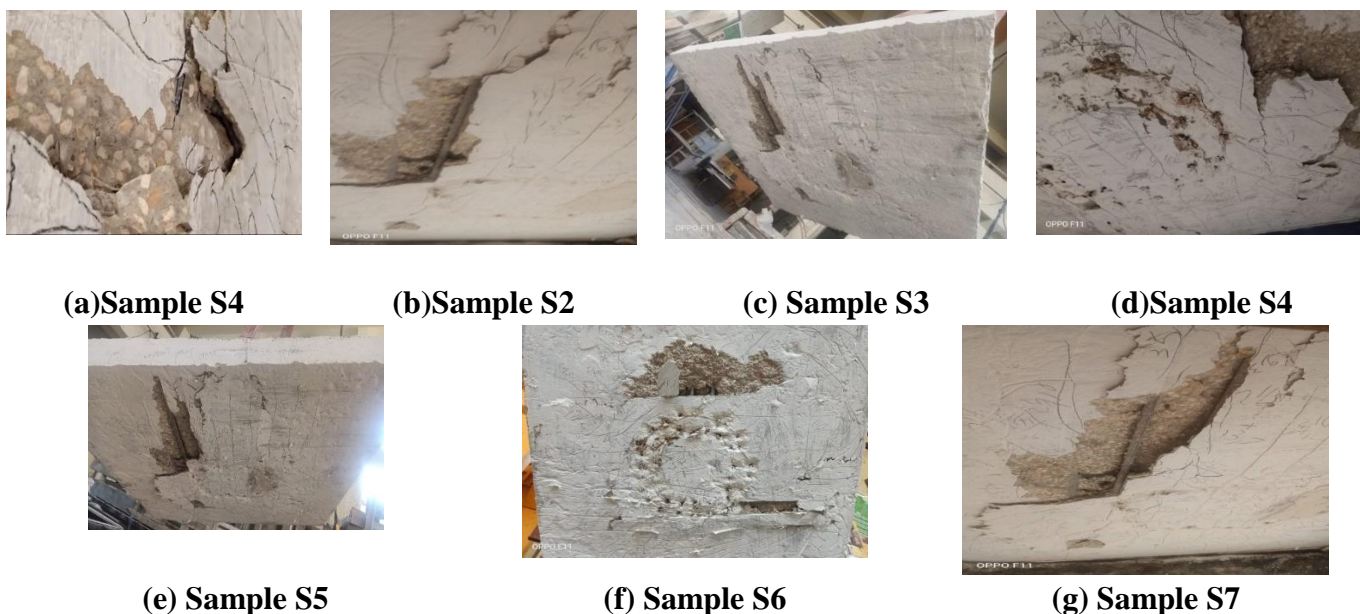


Figure 10 Failure modes of all tested specimens.

3.4 Ultimate load (P_u)

In general, there is raise in the ultimate load for all specimens with different proportions compared to the ultimate load of control (Specimen S1) as a result of the different methods used for external strengthened slabs.

The values of ultimate loads are displayed in Table 2 and the test results compared to the reference sample S1 are displayed in Table 3. The test results displayed that the ultimate load (P_u) was enhanced due to external strengthening, where the ultimate load (P_u) raise by 53%, 53%, 68%, 60%, 87% and 10% respectively for samples S2, S3, S4, S5, S6 and S7 compared to the reference sample S1. It is clear that, strengthen of slabs using two rows of external GFRP stirrups (Specimen S6) is the best method which gives raise in the ultimate load (P_u) and the deflection at ultimate load (Δ_u) by 87 % and 78 % respectively compared to the reference sample S1.

The use of two rows of steel shear studs (Bolts) is better than the use of one row, where raise in the ultimate load for one row and two rows of steel shear studs (Bolts) is 53 % and 68 % respectively compared to the control specimen S1, while these values are 60 % and 87 % for one row and two rows of GFRP stirrups.

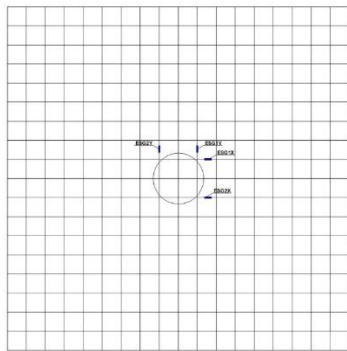
It can be noticed that using external drop panel confined with GFRP sheets (Specimen S2) and using steel shear studs (Bolts) (Specimen S3) on circle at distance $d/2$ from the column face improved the ultimate load almost with the same proportion 53% of the ultimate load. External strengthen using GFRP stirrups (Specimens S5 and S6) is better than external strengthen using steel shear studs (Bolts) (Specimen S3 and S4) has the same conditions. External strengthen using steel shear studs (Bolts) and GFRP stirrups at distance $d/2$ and d (Specimens S4 and S6) is better than using it at distance $d/2$ (Specimens S3 and S5).

It is recommended to use external strengthen using external reinforced concrete drop confined by GFRP sheets to get 53 % increase in the ultimate load where this method is the easier method and do not need professional techniques. It is recommended to use external strengthening using two rows of GFRP stirrups at distances $d/2$ and d from the column face to get 87 % raise in the ultimate load but this method needs drilling the slab and need professional technique and special tools. The use of GFRP sheets in the compression side of the slab (Specimen S7) is the worst method for strengthen which gives only 10 % increase in the ultimate load.

3.5 Load-strain curves

All electric strain gauges (ESG) were placed on the tension steel reinforcement layer as shown in Fig. 11. The experimental load– strain curves for the seven tested samples are plotted in Fig. 12. These figures show the measured strain of the main reinforcement in x and y directions. The average strain at the ultimate load in the main longitudinal steel reinforcement in x and y directions ϵ_1 and ϵ_2 respectively is shown in Table 2 for all tested samples. Table 3 shows the test results compared to the control sample S1. Generally, strain increased with increasing load until reached the ultimate load. It is observed the strain improved almost linearly with load until failure occurred.

From results, the yielding of longitudinal main reinforcement occurred at 98%, 92%, 93%, 88%, 91%, 85% and 97% of its ultimate load for samples S1, S2, S3, S4, S5, S6 and S7 respectively. For strengthened specimens S2, S3, S4, S5 and S6, the failure occurred after yielding of the main reinforcement then the flexural-punching mode of failure occurred. Therefore, the failure mode of specimens S1 and S7 is punching shear failure while the failure of the strengthened samples S2, S3, S4, S5 and S6 is flexural-punching failure.



- ESG1X and ESG2X at bottom mesh in the X direction for the first layer of reinforcement
- ESG1Y and ESG2Y at bottom mesh in the Y direction for the second layer of reinforcement

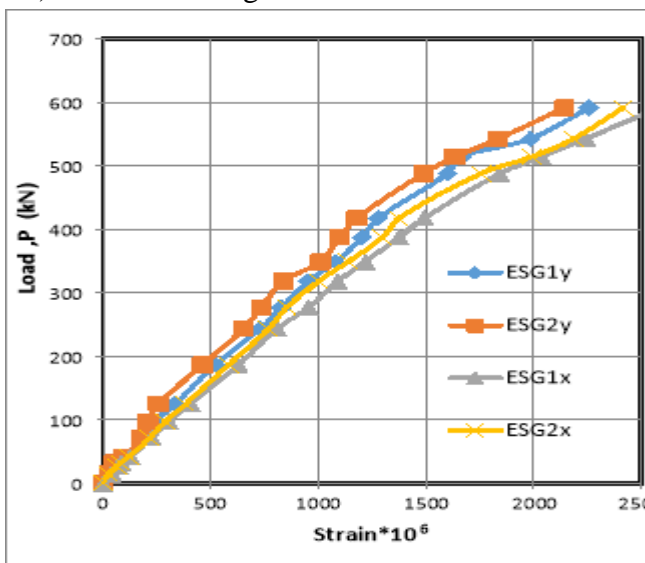


(a) Bottom steel reinforcement and electric strain gauges (ESG).

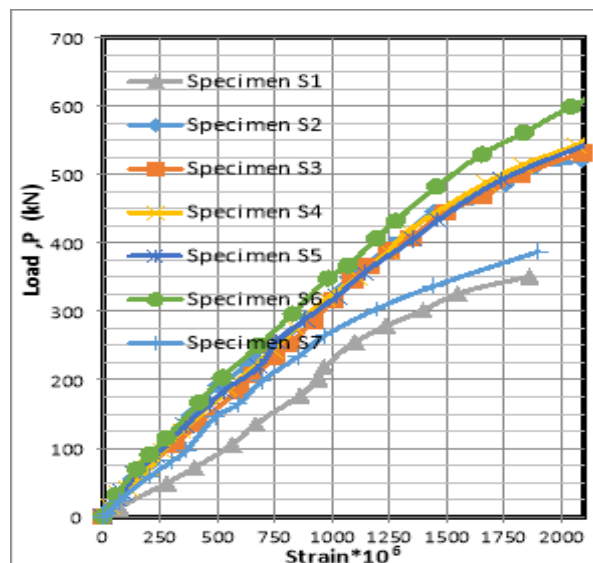
(b) Photo of the locations of the electric strain gauges (ESG).

Figure 11 Electric strain gauges (ESG) locations.

Furthermore, the strain in the main steel reinforcement in specimen with GFRP stirrups at a load level was less than that for samples with steel shear studs (bolts). Hence, it may be concluded that GFRP stirrups decrease the demand of the slab flexural reinforcement to resist punching shear. These results indicated that, GFRP stirrups effect on main steel reinforcement stresses and punching shear capacity. It is noticed, in the presence of the external GFRP stirrups on circles at distance $d/2$ and d from the column face (Specimens S6) decrease the strain in the main reinforcement compared to the case of GFRP stirrups on circle at distance $d/2$ (Specimen S5) as shown in Fig. 12.



(a) Specimen S4



(b) Load- Average Strain Curves of All

Specimens.

Figure 12 Load-strain curves.

3.6 Secant stiffness (S.S)

Utilizing tension reinforcement exhibit an enhancement in the secant stiffness (S.S) of the slabs as displayed in Table 2. The secant stiffness is enhanced for slabs S4, and S6 compared to the control specimen S1 by 5 % and 7 % respectively while for the specimen S2, S3, S5 and S7, the external strengthening has insignificant effect on secant stiffness (2%,0%,1.0 % and 0 % respectively).

3.7 Displacement Ductility (D.D)

The tests results compared to the control sample S1 showed in table 3. The displacement-ductility (D.D) increased by 3 %, 36 %, 27 %, 9 %, 9 % and 2 % for specimens S2 to S7 compared to the reference sample S1. The use of two rows of steel shear studs (Bolts) (Samples S3 and S4) and GFRP stirrups (Samples S5 and S6) on circles at distance $d/2$ and d are the most suitable methods for strengthen slabs for punching. The use of GFRP sheet in the compression side as external strengthen has insignificant effect in the displacement-ductility (2 %).

3.8 Toughness (T)

Toughness (T) is the ability of the specimen to adsorb deformations up to the ultimate load which equals the area down the load-deflection curve even the ultimate load (kN.mm). Therefore, it is a function of the ultimate load (P_u) and the corresponding ultimate deflection (Δ_u) as shown in Table 2 for all specimens. Toughness (T) is a good indication to measure the ductility of the slabs. In this study, toughness improved for all external strengthened slabs. The toughness was enhanced for slabs S2, S3, S4, S5, S6 and S7 by 140%, 82%, 154%, 211%, 316% and 35% respectively compared to the control specimen S1. The different methods used for external strengthen of slabs S2, S3, S4, S5 and S6 provided more ductile behavior, consequently, significant enhancement in the toughness was noticed. Finally, using external strengthen using GFRP stirrups on circles at distance $d/2$ and d from the column face is an effective method to enhance the toughness of the reinforced concrete flat slabs. A slight change in the toughness was noticed for slab S7 externally strengthen using GFRP sheets in the compression side.

4. Analytical Model

4.1 General

Generally, the design of flat slabs reinforced concrete is ruled by punching capacity of the slabs. In general, the slab thickness or the quantity and distribution of the shear reinforcement might differ between different nations and different codes. Because related reinforcement particulars and calculate punching shear capacity depend much more on the code applied.

4.2 Egyptian Code [1]

According to ECP (203-2017) [1] the punching shear of flat slab is Q_{uc} .

$$Q_{uc} = q_{cup} \cdot b \cdot d \quad (1)$$

where:

b_0 : the perimeter of the critical section located half the slab effective depth; d , from the face of the column as shown in Fig. 2;

q_{cup} : the ultimate shear stress carried by concrete only, which is the minimum value from Eqs. (2), (3) and (4);

$$q_{cup1} = 0.8 * [((\alpha.d)/b_0) + 0.2] * \sqrt{f_{cu}/\gamma_c} \quad (2)$$

$$q_{cup2} = 0.316 * [0.5 + (a/b)] * \sqrt{f_{cu}/\gamma_c} \quad (3)$$

$$q_{cup3} \leq 0.316 * \sqrt{f_{cu}/\gamma_c} \leq 1.7 \text{ MPa} \quad (4)$$

f_{cu} : the concrete cubic compressive strength after 28 days (MPa);

α : is a factor according the position of the column.

γ_c : is the strength reduction coefficient for concrete in compression; $\gamma_c=1.5$ for design and 1.0 for analysis; and

a and b : are the largest. and the smallest column dimensions for rectangular column and equal the column diameter for circular column.

The punching shear resistance using shear reinforcement calculated from Eq. (5)

$$Q_{uc} = q_{up} * b_0 * d \quad (5)$$

Where:

$$q_{up} = q_{cup} + q_{sup} = 0.12 \sqrt{f_{cu}/\gamma_c} + (A_{st} * f_y) / (S * b_0 * \gamma_s) \leq 0.45 * \sqrt{f_{cu}/\gamma_c} \quad (6)$$

4.3 ACI Code [2]

4.3.1 Two-way shear strength

Nominal shear strength for two-way members (slabs) without shear reinforcement (v_n) can be calculated by:

$$v_n = v_c \quad (7)$$

Nominal shear strength for two-way members (slabs) with shear reinforcement (v_n) can be calculated by:

$$v_n = v_c + v_s \quad (8)$$

Two-way shear can be resisted by a section with a depth d and an assumed critical perimeter b_0

For calculation of concrete contribution v_c and shear reinforcement contribution v_s for two-way shear, d can be taken as the average of the effective depths in the two orthogonal directions.

4.3.2 Two-way shear strength provided by concrete in slabs without shear reinforcement for non-prestressed two-way members

- v_c shall be calculated in accordance the least of Eqs. (9), (10) and (11):

$$0.33 k_s k \sqrt{f_c} \quad (9)$$

$$\left(0.17 + \frac{0.33}{\beta}\right) k_s k \sqrt{f_c} \quad (10)$$

$$\left(0.17 + \frac{0.083\alpha_s d}{b_0}\right) \lambda_s \lambda \sqrt{f'_c} \quad (11)$$

Where:

– λ_s ; the size effect factor given in $\lambda_s = \sqrt{\frac{2}{1 + 0.004d}} \leq 1$ (12)

– $\lambda = 1$ for normal weight concrete (13)

- f'_c : the concrete cylindrical strength (MPa);
- β : the ratio of long to short sides of the column rectangle, $\beta = 1$ for circular column;
- α_s : 40 for interior columns, 30 for edge columns, and 20 for corner columns; and
- The value of $\sqrt{f'_c}$ not exceed 8.3 MPa (f'_c not exceed. 68.89 MPa).

4.3.3 Two-way shear strength provided by concrete in members with shear reinforcement for two-way members (slabs) with shear reinforcement

- v_c at critical sections can be calculated in accordance to Table 4.

Table 4 Shear strength provided by concrete v_c

Type of shear reinforcement	Critical sections	v_c		Case
Stirrups	All	$0.17\lambda_s \lambda \sqrt{f'_c}$		(a)
Headed shear stud reinforcement	According to 22.6.4.1 ACI [2]	Least of (b), (c), and (d):	$0.25\lambda_s \lambda \sqrt{f'_c}$	(b)
			$0.17\left(1 + \frac{2}{\beta}\right) \lambda_s \lambda \sqrt{f'_c}$	(c)
			$0.83\left(2 + \frac{\alpha_s d}{b_0}\right) \lambda_s \lambda \sqrt{f'_c}$	(d)
	According to 22.6.4.2 ACI [2]	$0.17\lambda_s \lambda \sqrt{f'_c}$		(e)

Where: - For two-way shear, critical sections shall be located so that the perimeter b_0 is a minimum but need not be closer than $d/2$ to (a) and (b):

(a) Edges or corners of columns, concentrated loads, or reaction areas.

(b) Changes in slab or footing thickness, such as edges of capitals, drop panels, or shear caps.

-For a circular or regular polygon-shaped column, critical sections for two-way shear in accordance with cases (a) and (b) shall be permitted to be defined assuming a square column of equivalent area.

-For two-way members reinforced with headed shear reinforcement or single- or multi-leg stirrups, a critical section with perimeter b_0 located $d/2$ beyond the outermost peripheral line of shear reinforcement shall also be considered. The shape of this critical section shall be a polygon selected to minimize b_0 .

4.3.4 Two-way members (slabs) with shear reinforcement

Effective depth shall be selected such that v_u calculated at critical sections does not exceed the values in Table 5.

Table 5 Maximum punching shear strength at the critical sections

Type of shear reinforcement	Maximum v_u at critical sections	Case
Stirrups	$0.5\Phi\sqrt{f'_c}$	(a)
Headed shear stud reinforcement	$0.66\Phi\sqrt{f'_c}$	(b)

Φ : the strength reduction factor =0.75 for two-way shear.

4.3.5 Two-way shear strength provided by single- or multiple-leg stirrups.

- Single- or multiple-leg stirrups fabricated from bars or wires shall be permitted to be used as shear reinforcement in slabs and footings satisfying (a) and (b):

(a) d is at least 150 mm

(b) d is at least $16d_b$, where d_b is the diameter of the stirrups

- For two-way members with stirrups, v_s shall be calculated by:

$$v_s = \frac{A_v f_{yt}}{b_0 s} \quad (14)$$

where A_v is the sum of the area of all legs of reinforcement on one peripheral line that is geometrically similar to the perimeter of the column section, and s is the spacing of the peripheral lines of shear reinforcement in the direction perpendicular to the column face, f_{yt} is shear reinforcement yielding strength.

4.3.6 Two-way shear strength provided by headed shear stud reinforcement

Headed shear stud reinforcement shall be permitted to be used as shear reinforcement in slabs and footings if the placement and geometry of the headed shear stud reinforcement.

- For two-way members with headed shear stud reinforcement, v_s shall be calculated by:

$$v_s = \frac{A_v f_{yt}}{b_0 s} \quad (15)$$

Where: A_v is the sum of the area of all shear studs on one peripheral line that is geometrically similar to the perimeter of the column section, and s is the spacing of the peripheral lines of headed shear stud reinforcement in the direction perpendicular to the column face.

- If headed shear stud reinforcement is provided, $\frac{A_v}{s}$ shall satisfy:

$$\frac{A_v}{s} \geq 0.17 \sqrt{f'_c} \frac{b_0}{f_{yt}} \quad (16)$$

5. Numerical Analysis using ANSYS Program

5.1 General

The nonlinear finite element analysis was implemented using a computer program "ANSYS 19.0". The structural elements and material properties used to represent concrete and reinforcement steel based on the technical manual of ANSYS 19.0 [30] software. A correlative study dependent on the load-deflection response was adopted to fruition the numerical model with the results of experimental.

5.2 Geometry, finite element model, loads and boundary conditions

The slabs tested were identical appreciated using equal-size 3-D isoparametric elements (25*25*25 mm) Solid65 as shown in Fig.13. As shown in the figure the column stub was exemplified to simulate the real figure and dimensions of column stub for the slabs tested. The samples tested were analyzed as simply supported along the four sides to simulate the experimental set-up.

ANSYS V19 referring to technical manual [30], the three-dimensional isoparametric element Solid65 was approved to model the concrete elements. Solid65 element is capable of cracking in tension and crushing in compression. It is defined by eight nodal points each having three translational degrees of freedom x, y, and z (and no rotational deformations), along with a 2 x 2 x 2 Gaussian integration scheme which is used for the computation of the element stiffness matrix. The element can represent one solid material (concrete), and up to three impeded reinforcing bars with different material properties. Both linear and nonlinear responses of the concrete were included. For the linear stage, the concrete is assumed to be an isotropic material up to cracking. For the nonlinear, the concrete may undergo plasticity. Cracking may take place up to three orthogonal directions at each integration point. The software package "ANSYS V. 19.0" [30] allows steel reinforcement to be defined using the smeared reinforcement approach, in which the amount of reinforcement is defined by specifying a volume ratio and orientation angles of the rebar.

In this research, the reinforcing bars, steel shear studs and GFRP stirrups were idealized using a 2-node bar (linear) named element (Link 180). GFRP sheets in the compression side represented by element (Shell 181). The ultimate strength of the used GFRP sheets, GFRP stirrups and steel shear studs are 1100,1000 and 500 MPa respectively.

5.3 Material modeling

One of the main features of the concrete materials model is to predict the failure of brittle materials. Both cracking and crushing failure modes are involved.

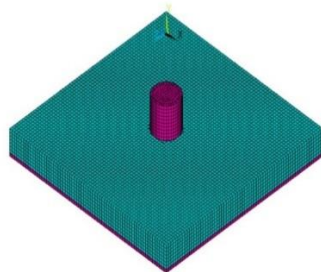
5.4 Solution techniques for numerical analysis and failure criteria

In the nonlinear analysis, the total load is divided into load steps which called load increments. When each incremental solution is completed, the stiffness matrix of the model changes before proceeding with the next load increment to reflect nonlinear alterations in structural stiffness.

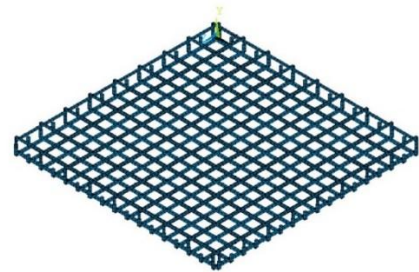
The signs of failure are more evident in the form of cracks pattern and the reaching of the concrete to its maximum strain.

5.5 Validation models

A comparison was through between the results of experimental and the results from ANSYS program to verify the numerical model, and it has been confirmed that there is a good estimated between the results. This is evident in Fig.14, which shows the relationship between the load - deflection of the tested beams and the numerical beams. Tables 6 and 7 show the ratio between the ultimate load and deflection at ultimate load for the tested slabs and the numerical slabs. The mean and standard deviation show a good agreement with the measured load – deflection and the calculated ones. Figure15 shows the predicted cracks pattern of the numerical models in comparison with Figure 4. A good estimated was observed between predicted cracks and measured cracks.



(a) Concrete elements (Solid 65)



(b) Reinforcing bar elements (Link 180)

Figure 13 ANSYS idealization of slabs S1 to S7.

5.6 Analysis of numerical results

The numerical results from finite element analysis and the results of experimental program at mid span are plotted in Fig. 14. Figure 16 shows the contours of the deflection (deformed shape) and the contours of the stresses for all tested slabs. Tables 6 and 7 present a comparison of the numerical cracking loads, ultimate loads and deflection at the ultimate load with the experimental results. As shown in Tables 6 and 7, the predicted cracking loads; $P_{cr Num.}$ are in general more than the observed experimental loads; $P_{cr exp.}$ with a mean ratio of $P_{cr Num.} / P_{cr exp.}$ 1.05 and a standard deviation (S.D) and a coefficient of variation (C.O.V) are 2 % and 0.02%

Good estimation between the results of experimental program and the nonlinear finite elements analysis was attained. The ratio between the numerical and the ultimate loads of experimental program; $P_{u Num.} / P_{u exp.}$ is shown in Table 7 which ranged between 1.03 and 1.07, with a mean value of 1.05, S.D and C.O.V 2.0% and 0.03 % respectively. The ratio between the numerical and the ultimate deflection of experimental program; $\Delta_{u Num.} / \Delta_{u exp.}$ is indicated in Table 7 which ranged between 0.85 and 1.34, with a mean value of 1.14, S.D and C.O.V 2%. and 2.66 % respectively. Furthermore, the analysis reverses the importance of the tested parameters verification including good effect of steel shear studs and GFRP stirrups on cracking and ultimate load.

The Nonlinear Finite Element Analysis NLFEA gave a good agreement for centripetal deflection during the different loading stages of most the tested samples, while failed to forecast the post-peak behavior for some samples tested specially those undergo sudden punching failure.

The mean predicted-to-experimental cracking, ultimate load and deflection at ultimate load are 1.05, 1.05 and 1.14 respectively with (C.O.V) 0.02%, 0.03 % and 2.66%. the method of applying load is a basic method for all expectation.

Also, the results showed that both ECP 203-2017 [1] and ACI 318-19 [2] building codes are conservative compared to the results of experimental program displayed in Tables 6 and 7. The comparison between ECP 203-2017 [1] and ACI 318-19 [2] codes with experimental and numerical ultimate loads shows a important variation in the punching shear calculations according to codes. The Egyptian code ECP 203-2017 [1] is conservative compared to ACI 318-19 [2] where the mean, S.D and C.O.V of $P_{u \text{ Egyptian Code}} / P_{u \text{ ACI}} \%$ are 94 %, 7 % and 0.48 %.

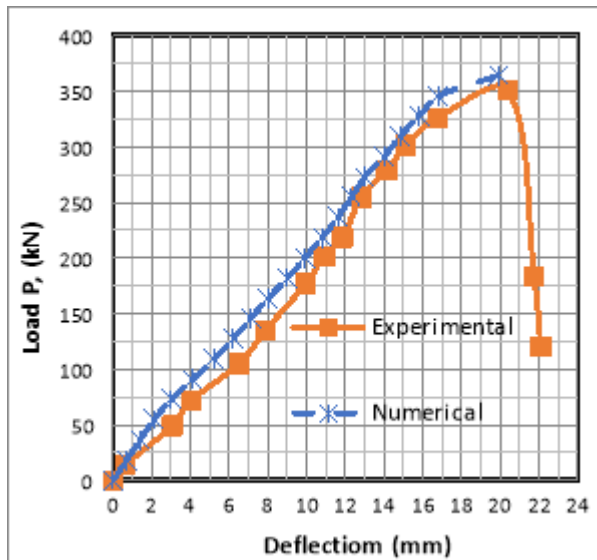
Table 6 Predicated results from finite element and codes.

Specimen No.	Results of Experimental Programe			finite element results			Codes results	
	Crackin g load $P_{cr \text{ exp.}}$ (kN)	Ultimat e load $P_{u \text{ exp.}}$ (kN)	Deflectio n at ultimate load $\Delta_{u \text{ Exp.}}$ (mm)	Crackin g load $P_{cr \text{ Num}}$ (kN)	Ultimat e load $P_{u \text{ Num.}}$ (kN)	Deflectio n at ultimate load $\Delta_{u \text{ Num.}}$ (mm)	P_u Egyptian [1] (kN)	$P_{u \text{ ACI}}$ [2] (kN)
S1	135.18	351.01	20.386	140	364	19.92	249.94	240.09
S2	191.35	535.63	30.485	205	570	35.33	568.82	549.60
S3	184.85	536.12	31.056	190	550	37.06	335.44	366.17
S4	243.58	591.10	32.651	255	630	27.79	420.95	459.51
S5	183.45	562.37	32.374	190	590	42.79	335.44	366.17
S6	250.37	657.29	36.293	260	700	48.61	420.95	459.51
S7	146.12	387.08	22.455	155	415	25.84	335.44	404.37

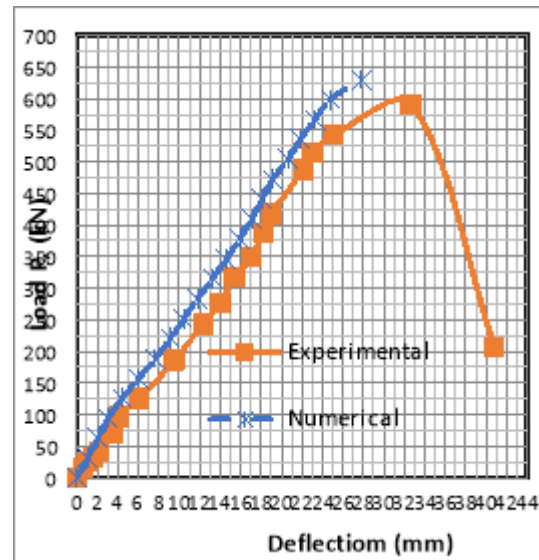
Table 7 Comparison between experimental, numerical and analytical results.

Slab No.	S1	S2	S3	S4	S5	S6	S7	Mean	Standard deviation (S.D)	Coefficie nt of variation (C.O.V)
$P_{cr \text{ FE}} / P_{cr \text{ exp.}}$	1.04	1.07	1.03	1.05	1.04	1.04	1.06	1.05	0.02	0.02 %
$P_{u \text{ FE}} / P_{u \text{ exp.}}$	1.04	1.06	1.03	1.07	1.05	1.06	1.07	1.05	0.02	0.03 %
$\Delta_{u \text{ FE}} / \Delta_{u \text{ exp}}$	0.98	1.16	1.19	0.85	1.32	1.34	1.15	1.14	0.02	2.66 %

$P_{u \text{ Egyptian [1]}} / P_{u \text{ exp.}}$	0.71	1.06	0.63	0.71	0.60	0.64	0.87	0.75	0.17	2.35 %
$P_{u \text{ ACI [2]}} / P_{u \text{ exp.}}$	0.68	1.03	0.68	0.78	0.65	0.70	1.04	0.80	0.17	2.44 %
$P_{u \text{ Egyptian [1]}} / P_{u \text{ ACI [2]}}$	1.04	1.03	0.92	0.92	0.92	0.92	0.83	0.94	0.07	0.48 %



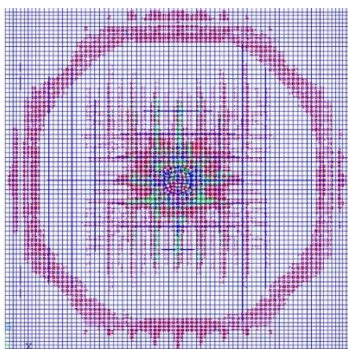
(a) Specimen S1



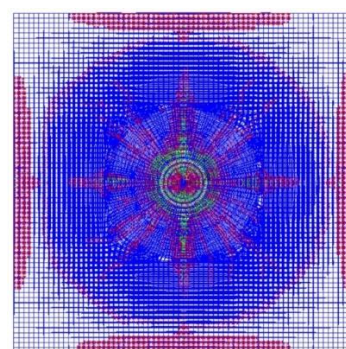
(d) Specimen S4

Figure 14 Experimental and numerical load-deflection curves.

Figure 16 shows both experimental and numerical (FE) results indicating the cracks propagation. From this figure, it can be noticed that, all the measured and the predicted cracks patterns are similar.

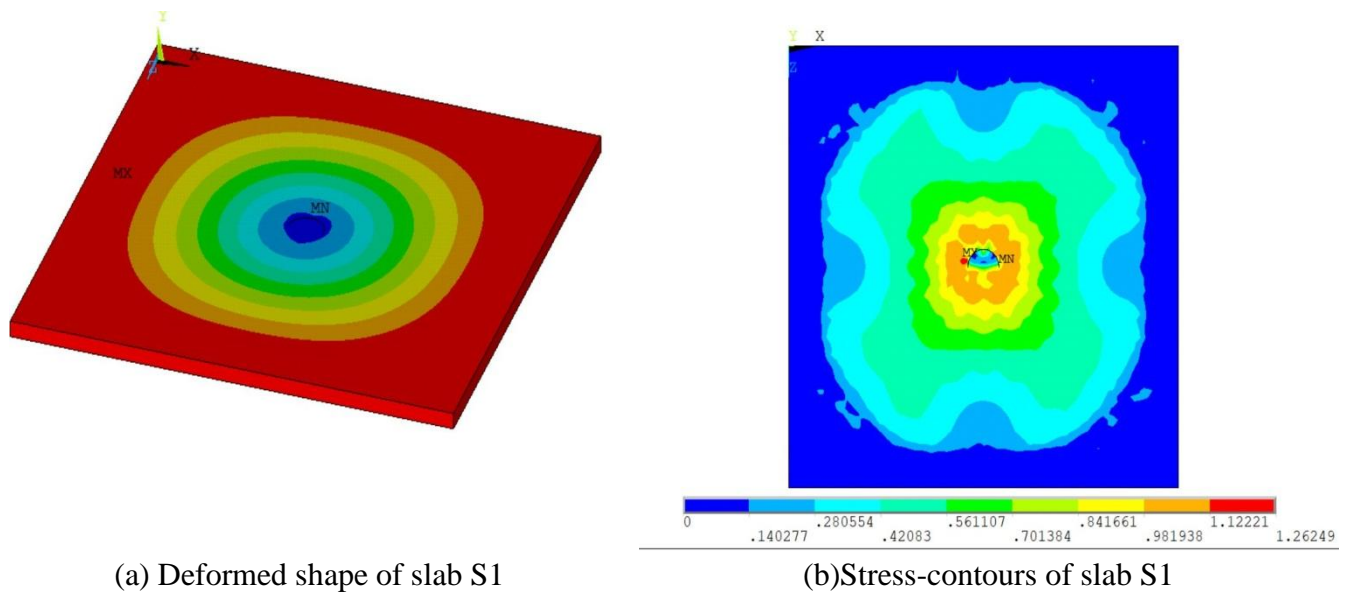


(a) Specimen S1



(d) Specimen S4

Figure 15: Numerical cracks propagation.



(a) Deformed shape of slab S1

(b) Stress-contours of slab S1

Figure 16 Deformed shapes and stress contours.

6 Conclusions

- 1- The ultimate load is enhanced due to external strengthening of the reinforced concrete flat slabs.
- 2- The external strengthening increases the deflection at the first and second crack which means increase the secant stiffness (load/deflection) and increase displacement ductility and toughness.
- 3- The external strengthening has low influence on the secant stiffness of the reinforced concrete flat slabs.
- 4- The methods used for external strengthening of the slabs provided more ductile behavior, hence, significant enhancement in the toughness was noticed.
- 5- It is recommended to use external strengthen using reinforced concrete drop panel confined by GFRP sheets to get 53 % increase in the ultimate load where this method is the easier method and do not need professional techniques.
- 6- The use of external drop panel confined with GFRP sheets and using steel shear studs (Bolts) on circle at distance half the slab effective depth from the column face improved the ultimate load almost with the same proportion (53% of the ultimate load of the un-strengthened slab).
- 7- Strengthened slabs using two rows of external GFRP stirrups is the best method which gives an raise in the ultimate load and the corresponding deflection, secant stiffness, displacement ductility and toughness by 87 % ,78 % , 7%, 9 % and 316% respectively compared to the unstrengthen sample.
- 8- It is recommended to use external strengthen using two rows of GFRP stirrups on circles at distance half the slab effective depth and at the slab effective depth from the column face to get 87 % raise in the ultimate load but this method needs drilling the slab and need professional technique and special tools.
- 9- The use of external strengthen by GFRP stirrups on circles at distance half slab effective depth and slab effective depth from the column face is an effective method

to improve the toughness of the reinforced concrete flat slabs. A slight change in the toughness was noticed for slab externally strengthened using GFRP sheets in the compression side.

- 10- External GFRP stirrups effect on main steel reinforcement stresses and punching shear capacity.
- 11- Using external strengthen by GFRP stirrups on circles at distance half the effective slab depth and at the effective slab depth from the column face is an effective method to enhance the toughness of the reinforced concrete flat slabs.
- 12- The use of GFRP stirrups decrease the contribution of the slab flexural reinforcement to resist punching shear. These results indicated that, GFRP stirrups effect on main steel reinforcement stresses and punching shear capacity.
- 13- The external strengthening using steel shear studs (Bolts) and GFRP stirrups changed the failure type from punching failure mode to flexural – punching failure mode with some warnings.
- 14- The use of GFRP stirrups instead of steel shear studs (Bolts) is better not only in resisting punching but also in reducing deflection, cracks width and cracks propagation.
- 15- The use of two rows of steel shear studs (Bolts) is better than the use of one row, where the increase in the ultimate load for one row and two rows of steel shear studs (Bolts) is 53 % and 68 % respectively compared to the unstrengthen slab, while these values are 60 % and 87 % for one row and two rows of GFRP stirrups.
- 16- External strengthen using GFRP stirrups is better than external strengthen using steel shear studs (Bolts) has the same conditions.
- 17- External strengthening using steel shear studs (Bolts) and GFRP stirrups on circles at distance half the slab effective depth and at the slab effective depth is better than using it on a circle at distance half the slab effective depth.
- 18- The use of two rows of steel shear studs (Bolts) and GFRP stirrups on circles at distance half the slab effective depth and at the slab effective depth are the most effective method for strengthen slabs for punching.
- 19- The first and the second crack load for specimens strengthened using steel shear studs range between 37 % to 92 % of the ultimate load while these values ranging between 40 % to 101 % for specimens strengthened using GFRP stirrups.
- 20- Using of two rows of steel shear studs (Bolts) or GFRP stirrups effectively prevent propagation of shear cracks and reduce crack width compared to the specimen using one row.
- 21- The use of steel shear studs (Bolts) and GFRP stirrups on circles at distance half slab effective depth and at distance half slab effective depth and the slab effective depth from the column face change the failure mode from punching failure to punching-flexural failure.
- 22- There was significant improvement in the maximum deflection recorded for slabs with GFRP stirrups or steel shear studs (bolts) before failure compared to the unstrengthen specimen.

- 23- The use of GFRP stirrups instead of steel shear studs (Bolts) is better not only in resentencing punching but also in reducing the deflection, cracks width and cracks propagation.
- 24- External strengthen using GFRP stirrups is better than external strengthen using steel shear studs (Bolts) has the same conditions.
- 25- External strengthen using steel shear studs (Bolts) and GFRP stirrups at distance half the effective slab depth and at the effective slab depth is better than using it at distance half the effective slab depth.
- 26- The use of GFRP sheets in the compression side of the slab is the worst method for strengthening which gives only 10 % raise in the ultimate load.
- 27- The use of GFRP sheet in the compression side as external strengthen has insignificant effect in the displacement-ductility (2 %).
- 28- The use external GFRP sheets in the compression side gives insignificant enhancement for the first, second crack, yielding and ultimate load.
- 29- Good agree between the experimental results and the nonlinear finite elements analysis was achieved.
- 30- The nonlinear finite element analysis gives good estimate of central deflection through the loading phases for most of the tested samples.
- 31- The numerical analysis defeated in expect the post-peak behavior for certain tested samples.
- 32- The numerical analysis sufficiently reflects the improvement in the punching shear capacity logged for slabs provided with steel shear studs and GFRP stirrups.
- 33- The mean of the predicted-to-experimental the cracking load, ultimate load and deflection at ultimate load are 1.05,1.05 and 1.14 respectively with coefficient of variation (C.O.V) 0.02%, 0.03 % and 2.66%.
- 34- The results show that ECP 203-2017 [1] is conservative compared to ACI 318-19 [2] where the mean, S.D and C.O.V of $P_{u \text{ Egyptian Code}} / P_{u \text{ ACI}}$ equal % are 94 %,7 % and 0.48 %.

References

- [1] Egyptian Code of Practice for Design and Construction of Reinforced Concrete Structures ECP-203, Housing and Building Research Center, Ministry of Building and Construction, Giza, Egypt, 2017, Chapter 6, pp. 113-122.
- [2] ACI Committee 318-19, Building Code Required for Reinforced Concrete, (ACI 318-19) and Commentary (ACI 318R-19), American Concrete Institute, Farmington Hills, Mich,2019, Chapter 22, 4011-420
- [3] Hazem, M.F., and Elbakry, S. M.A., “Punching strengthening of two-way slabs using external steel plates”, Alexandria Engineering Journal, Vol.54, pp.1207-1218, 2015.
- [4] Ismail, G., Abdel-Karem, A., Debeiky, A., and Makhlof, M. “Strengthening and repair of reinforced concrete slab-column connection subjected to punching shear using (CFRP - GFRP - Steel) Stirrups”, ICSSD 2012, Fourth International Conference on Structural Stability and Dynamics, India, 2012.

- [5] Khaleel, G.I., Shaaban, I.G., Elsayed, K.M., and Makhlof, M.H., “Strengthening of reinforced concrete slab-column connection subjected to punching shear with FRP systems”, International Conference on Civil and Architecture Engineering, Barcelona, Spain, 2013 and International Journal of Engineering and Technology (IJET), August, 2013.
- [6] Hasan, M. M., Mostofinejad, D., and Nakamura, H., “Strengthening of flat slabs with FRP fan for punching shear”, Composite Structures, Vol 119 (2015) pp305-314
- [7] Hasan, M.M., Davood, M., Hakru, N., and Mohammad, H. M., “Strengthening of flat slabs with FRP fan for punching shear”, Journal of Composite Structures, Vol. 119 ,2015, pp.305-314, 2014.
- [8] Eom, T. S., Kang, S. M., Choi, T. W., and Park, H. K., “Punching shear tests of slabs with high-strength continuous hoop reinforcement”, ACI Structural Journal, 115(5), 2018.
- [9] Zhu, Y., Zhang, Y. Hussein, H.H. and Chen, G., “Flexural strengthening of reinforced concrete beams or slabs using ultra-high-performance concrete, (UHPC): a state-of-the-art review”, Engineering. Structures. 205, 110035, 2020.
- [10] Eid, F. M., “New methods for resisting punching shear stress in reinforced concrete flat slabs ”, Journal of Current Engineering and Technology, Vol.8, no.2, March/April,2018.
- [11] Rasha, T.S. M., “Effect of flexural and shear reinforcement on the punching behavior of reinforced concrete flat slabs”, Alexandria Engineering Journal, Vol. 56, 2017.
- [12] Jae, I.J. and Su, M. K., ‘ “Punching shear behavior of shear reinforced slab– column connection with varying flexural reinforcement”, International Journal of Concrete Structures and Materials, ,2019.
- [13] Lips, S., Fernandez, M.R. and Muttoni, A., “Experimental investigation on punching strength and deformation capacity of shear-reinforced slabs”, ACI Structural Journal,109(1): 889–900, 2012.
- [14] Pop, A., “Punching shear capacity of reinforced concrete slabs with transverse reinforcement”, Master Thesis, Department of Civil Engineering, Technical University of Denmark, Lyngby, Denmark, 2014.
- [15] Hamed, S.A., “Repair of RC flat plates failing in punching by vertical studs”, Alexandria Engineering Journal, 2015.
- [16] Thai, X. D. and James, K.I. W., “Flexurally-triggered punching shear failure of reinforced concrete slab-column connections reinforced with headed shear studs arranged in orthogonal and radial layouts”, Engineering Structures ,12120 pp.258-268, 2016.
- [17] Nasr, Z.H., and Mostafa, A.O., “Enhancement of punching shear strength of flat slabs using shear band reinforcement”, Housing and Building National Research Center, Vol. 14, pp. 393-399, 2017.
- [18] Padmanabham, K., “Punching shear improvement of flat slabs using steel fibers and shear studs”, International Journal of Civil Engineering and Technology (IJCIET), Vol. 10, Issue 11, November 2019.
- [19] Joaquim, A.O., Barros, B. N., Moraes, N., Guilherme, S.S.A., and Cristina, M.V.F., “Assessment of the effectiveness of steel fiber reinforcement for the punching resistance of flat slabs by experimental research and design approach”, Computers Part B 78, pp.8-25, 2015.

- [20] Nasr, Z.H., and Ahmed, M. A., “Punching shear behavior of reinforced concrete using steel fibers in the mix”, Housing and Building National Research, Vol. 14, pp.272-281, 2018.
- [21] Moreno, C.L. and Sarmiento, A.M., “Punching shear analysis of slab–column connections”, Engineering Computations, 30(6): 802–814, 2013, 2013.
- [22] Mikcallef, K., Sagaseta, J., Fernandez, M. and Ruiz, A.M., “Assessing punching shear failure in reinforced concrete flat slabs subjected to localized impact loading”, International Journal of Impact Engineering, 71, pp.17-33, 2014.
- [23] Aikaterini, S.G., and Maria A. P., “Finite element analysis of punching shear of concrete slabs using damaged plasticity model in ABAQUS”, Engineering Structures, 98, pp.38-48, 2015.
- [24] Malena, B. M., and Eugen, B., “Composite model for predicting the punching resistance of R-UHPFRC-RC composite slabs”, Engineering Structures, 117, pp.603-616, 2016.
- [25] Santhi, A.S., “Experimental study on behavior of flat slab under different support conditions”, International Journal of Pure and Applied Mathematics, Vol. 119 (12), 2018.
- [26] Long, N., Minh, M., Rovnak, T., Tran, N., and Them, L. P., “Punching shear resistance of post tensioned steel fiber reinforce concrete flat plates”, Engineering Structures 45 pp.324-337, 2012.
- [27] Robbert, K., A.K., and Thomas, K., “Punching shear strengthening of flat slabs using prestressed carbon fiber-reinforced polymer straps”, Engineering Structures, 76, pp.283-294, 2014.
- [28] ANSYS V.19 43- ANSYS, “Engineering Analysis System User's Manual, Vol. 1 and 2, and Theoretical Manual,” Revision 5.4, Swanson Analysis System Inc., Houston, Pennsylvania, 1999.